Intermolecular Forces in Organic Clusters

Michael Meot-Ner (Mautner)

Contribution from the Chemical Kinetics and Thermodynamics Division, National Institute of Standards and Technology, Gaithersburg, Maryland 20899. *Received July 15, 1991*

Abstract: The effects of alkyl groups on the binding energies of cluster ions were investigated. The data were obtained by variable-temperature pulsed high-pressure mass spectrometric equilibrium measurements on protonated clusters A_nH^+ (A = MeOH, *n*-PrOH, *n*-AmOH, MeCOOH, $MeNH_2$, *n*-$PrNH_2$, and Me_2NH). Inner shell binding energies are not affected by alkylation, suggesting pure hydrogen-bonding interactions with the core ions. Shell-filling effects are also not affected. Thus, going to the second shell causes an equal drop of 17 ± 4 kJ/mol (4 ± 1 kcal/mol) in all the observed clusters, despite the variation in the number of hydrogen-bonding sites and charge densities at the core ions. This suggests opposing effects of intramolecular and intermolecular solvation at the shell-filling step. However, the alkyl groups do affect the outer shells. The bonding energies in the outer shells of the alcohol clusters approach the respective bulk condensation energies within ±6 kJ/mol (±1.5 kcal/mol). This suggests liquidlike hydrophobic alkyl-alkyl interactions in the outer shells which may contribute 12-25 kJ/mol (3-6 kcal/mol) to the bonding energies.

Introduction

Protonated organic species interact strongly with solvent and solute molecules in the condensed phase. These interactions involve ionic hydrogen bond networks, as well as hydrophobic interactions of alkyl groups with the solvent. The contributions of these solvation factors were quantified using cluster thermochemistry and a continuum dielectric model.[1] The analysis showed that alkyl group interactions with the solvent contribute up to 25-145 kJ/mol (6-35 kcal/mol) to the solvation energies.[1]

The significance of alkyl and aryl group interactions was also observed in dimer ions of large molecules, where such interactions contribute up to 20 kJ/mol (5 kcal/mol) to the bonding energies in hydrogen-bonded dimers,[2] and up to 60 kJ/mol (14 kcal/mol) in aromatic dimer ions.[3] Alkyl group interactions can also lead to substantial entropy effects, with entropies of dimerization as large as -230 J/(mol K) (-55 cal/(mol K)) in alkylamines and alkylpyridines.[4] Kinetically, alkyl group interactions lead to slow proton transfer or hydride transfer in hindered alkylated systems.[5,6]

These observations show that alkyl group interactions are significant in dimer ions, as well as in bulk solution. This work will deal with alkyl group interactions in large clusters, where many such groups can interact.

Alkyl substitution can affect the clusters because of changes in the number of hydrogen-bonding sites, charge densities, steric effects,[4] and dispersive hydrophobic bonding.[3] We observe the resulting trends with increasing cluster size in complex alkylated molecules, and compare them with more simple molecules.

The large clusters can be observed only near condensation, over a limited temperature range where the cluster distributions are broad and the concentration of each cluster is small. The resulting limitations on measurement will be analyzed.

Experimental Section

The measurements were done using the NIST pulsed high-pressure mass spectrometer.[4] Mixtures of alcohols or amines in N_2 or CH_4 carrier gas were prepared in a bulb heated to 180 °C, and allowed to flow to the ion source. Using N_2 was advantageous at low temperatures, since $C_2H_5^+$ and other ions in methane associate with amines and water and form cluster sequences that may present mass coincidence problems.

The pressure of the carrier gas in the ion source was 1-4 mbar, and that of the alcohols or amines was 0.01-0.001 mbar. Trace amounts of $CHCl_3$ were also added for electron capture to increase the ion residence times. The mixtures were ionized by 0.5-1-ms pulses of 500-1000-eV electrons. The distribution of cluster ions was observed for 1-4 ms after the pulse. The ion source was heated by heaters embedded in the walls, or cooled by liquid nitrogen flowing through channels in the source walls. The temperature was monitored by a copper-constantan thermocouple pressed under a copper plate near the ion exit pinhole. A detailed description of the source and of recent temperature calibrations is given elsewhere.[7]

The measurements were limited by the decomposition of protonated alcohols at high temperatures,[8] by condensation at low temperatures, and by the mass range of our instrument ($m/z < 700$). Measurements on $(n\text{-PrOH})_2H^+$, $(n\text{-AmOH})_2H^+$, and $(n\text{-AmOH})_3H^+$ were prevented by the pyrolysis of the protonated alcohols at high temperatures, with the loss of H_2O. The pyrolysis products are observed at the present low partial pressures of the alcohols, $<10^{-4}$ mbar, where their reactions with the parent molecules are slow. In *n*-PrOH, pyrolysis leading to the $C_3H_7^+$ ion is observable under such conditions, and we also observed the $C_3H_5OH_2^+$ ion above 470 K. The latter may be due to pyrolytic H_2 loss from the neutral molecule in the heated source, as was suggested recently by Stone.[8] Because of the pyrolysis problem, the equilibrium that forms $(n\text{-PrOH})_2H^+$ could not be measured directly. However, we obtained the thermochemistry using switching reactions in a mixture of 0.05% CD_3CN and 0.02% *n*-PrOH in N_2. These measurements can be done at low temperatures where the pyrolysis is negligible. Even when the formation of the dimers is irreversible, switching reactions among $(CD_3CN)_2H^+$, $(CD_3CN{\cdot}n\text{-PrOH})H^+$, and $(n\text{-PrOH})_2H^+$ are in equilibrium.

The monomer ion $n\text{-AmOH}_2^+$ was not observed under any conditions. The major ion observed above 380 K in mixtures containing *n*-AmOH was $C_5H_{11}^+$, and the H_2 loss product $C_5H_9OH_2^+$ was also observed as a minor peak. Below 360 K, the ion $(C_5H_{11})_2OH^+$ was formed. This may be due to the association of $C_5H_{11}^+$ with the parent molecules. This process, followed by clustering and switching reactions, could be a mechanism that forms the clusters $(n\text{-AmOH})_nH^+$.

Cluster peak intensities containing amines dropped abruptly at about 180-200 K, and those containing MeOH, *n*-PrOH, and *n*-AmOH at about 180, 210, and 220 K, respectively. This signaled that the samples condensed on the ion source walls or at cold spots near the liquid nitrogen coolant channels. Near the condensation temperatures, some systems such as MeOH below 200 K may have been supersaturated. Measurements on acetic acid clusters presented a further problem in that the neutral vapor dimerizes, leading to unreasonable results below 240 K. Other hydrogen-bonding neutrals may also dimerize in the gas phase near condensation. This adds to the uncertainty of measurements.

The reagents were commercial samples without further purification. Methylamine contained dimethylamine and trimethylamine impurities, apparently at levels of 1% and 0.1%, respectively. The impurities could not be removed by vacuum distillation, and the impurities prevented measurements at high concentrations of methylamine.

Results

The thermochemistry of the clustering reactions was obtained from van't Hoff plots, Figures 1-6. The results are reported in Table I.

(1) Meot-Ner (Mautner), M. *J. Phys. Chem.* **1987**, *91*, 417.
(2) Meot-Ner (Mautner), M. *Acc. Chem. Res.* **1984**, *17*, 186.
(3) Meot-Ner (Mautner), M. *J. Phys. Chem.* **1980**, *84*, 2724.
(4) Meot-Ner (Mautner), M.; Sieck, L. W. *J. Am. Chem. Soc.* **1983**, *105*, 2965.
(5) Meot-Ner (Mautner), M.; Solomon, J. J.; Field, F. H.; Gershinowitz, H. *J. Phys. Chem.* **1974**, *78*, 1733.
(6) Sunner, J.; Hirao, K.; Kebarle, P. *J. Phys. Chem.* **1989**, *93*, 4010.
(7) Meot-Ner (Mautner), M.; Sieck. L. W. *J. Am. Chem. Soc.* **1991**, *113*, 4448.
(8) Stone, J. *Int. J. Mass Spectrom. Ion Processes* **1991**, *104*, 95.
(9) Keesee, R. G.; Castleman, A. W. *J. Phys. Chem. Ref. Data* **1986**, *15*, 1011.
(10) El-Shall, M. S.; Meot-Ner (Mautner), M.; Sieck, L. W. *J. Phys. Chem.*, submitted for publication.

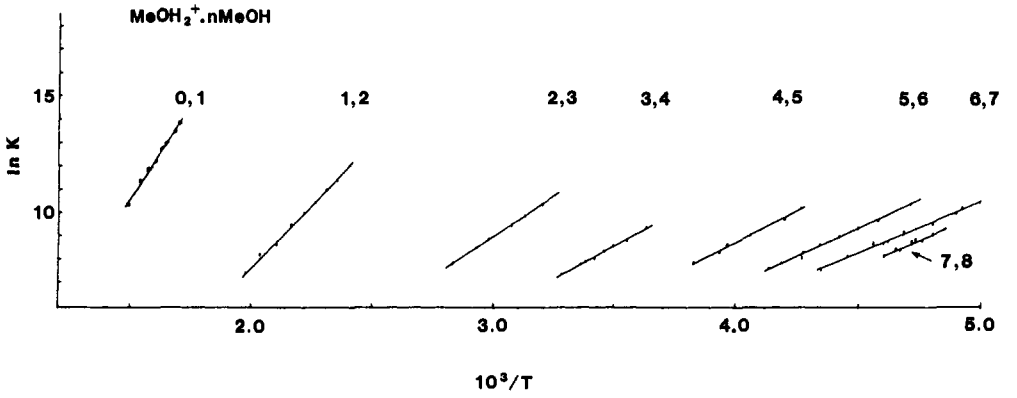

Figure 1. Van't Hoff plots for $BH^+\cdot(n-1)B + B \rightarrow BH^+\cdot nB$, for B = MeOH and $n - 1$, n as shown. K is in units of inverse bars.

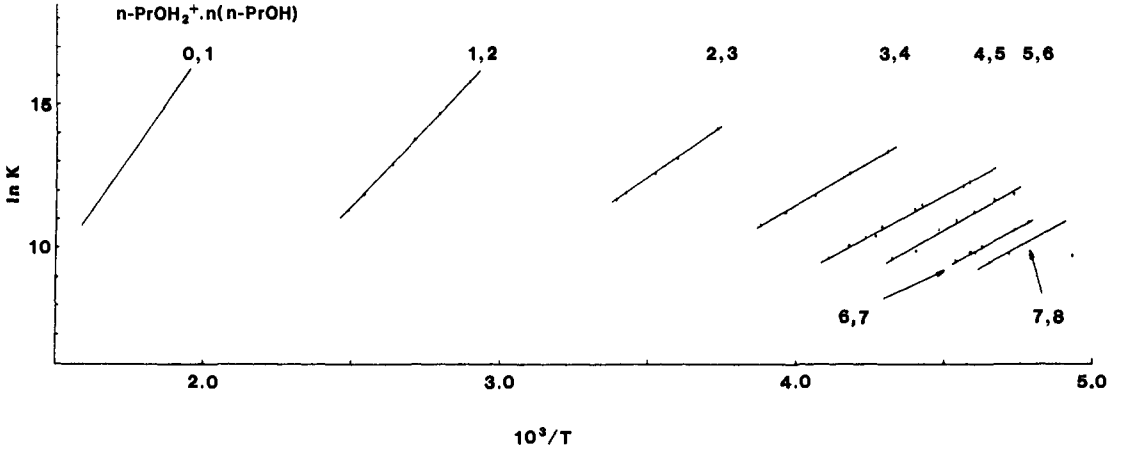

Figure 2. Van't Hoff plots as in Figure 1, for B = *n*-PrOH. The plot for the 0, 1 equilibrium is based on the thermochemistry from switching reactions, and for the 7, 8 equilibrium on the points shown and estimated $\Delta S°$; see Table I and text.

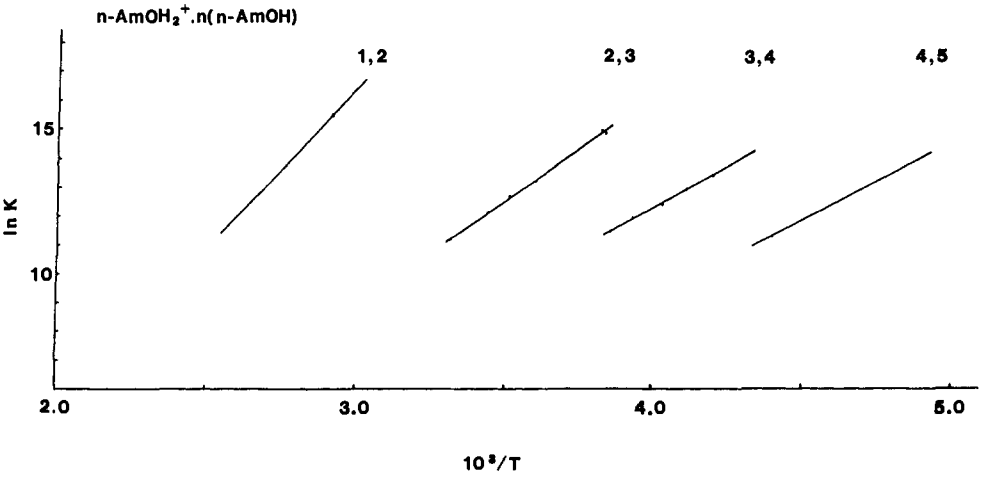

Figure 3. Van't Hoff plots as in Figure 1, for B = *n*-AmOH. The plots for the 1, 2 and 4, 5 reactions are based on the points shown and estimated $\Delta S°$; see Table I and text.

The $(MeOH)_nH^+$ clusters, up to $n = 8$, were measured in the presence of MeCN. Thermochemical cycles involving $(MeOH)_nH^+$ and $(MeCN)(MeOH)_{n-1}H^+$ mixed clusters, and reproducibility in duplicate measurements, were consistent within ±1.2 kJ/mol (±0.3 kcal/mol) in $\Delta H°$ and ±4 J/(mol K) (±1 cal/(mol K)) in $\Delta S°$. Also, 9 of the temperature studies on amines were duplicated with reactant concentrations varying up to a factor of 5. The average difference between duplicate results was 1 kJ/mol (0.3 kcal/mol) in $\Delta H°$ and 3 J/(mol K) (0.8 cal/(mol K)) in $\Delta S°$. Similar error estimates result from the standard deviations of the slopes and intercepts of the van't Hoff plots. Allowing for systematic errors, our error estimates are the usual values of ±4 kJ/mol (±1 kcal/mol) for $\Delta H°$ and ±8 J/(mol K) (±2 cal/(mol K)) for $\Delta S°$.

(11) Grimsrud, E. P.; Kebarle, P. *J. Am. Chem. Soc.* **1973**, *95*, 7939.
(12) Meot-Ner (Mautner), M. *J. Am. Chem. Soc.* **1986**, *108*, 6189.
(13) Hiraoka, K.; Morise, K.; Nishijima, T.; Nakamura, S.; Nakazato, M.; Ohkuma, K. *Int. J. Mass Spectrom. Ion Processes* **1986**, *68*, 99.
(14) Grimsrud, E. P.; Kebarle, P. *J. Am. Chem. Soc.* **1973**, *95*, 7939.
(15) Meot-Ner (Mautner), M. *J. Am. Chem. Soc.* **1984**, *106*, 1257.
(16) Lau, Y. K.; Saluja, P. S.; Kebarle, P. *J. Am. Chem. Soc.* **1980**, *102*, 7429.
(17) Hiraoka, K.; Takimoto, H. *J. Phys. Chem.* **1986**, *90*, 5910.
(18) Yamdagni, R.; Kebarle, P. *J. Am. Chem. Soc.* **1973**, *95*, 3504.
(19) Holland, P. M.; Castleman, A. W. *J. Chem. Phys.* **1982**, *76*, 4195.
(20) Meot-Ner (Mautner), M.; Sieck, L. W. *J. Am. Chem. Soc.* **1983**, *105*, 2956.
(21) Meot-Ner (Mautner), M. *J. Am. Chem. Soc.* **1979**, *101*, 2396.

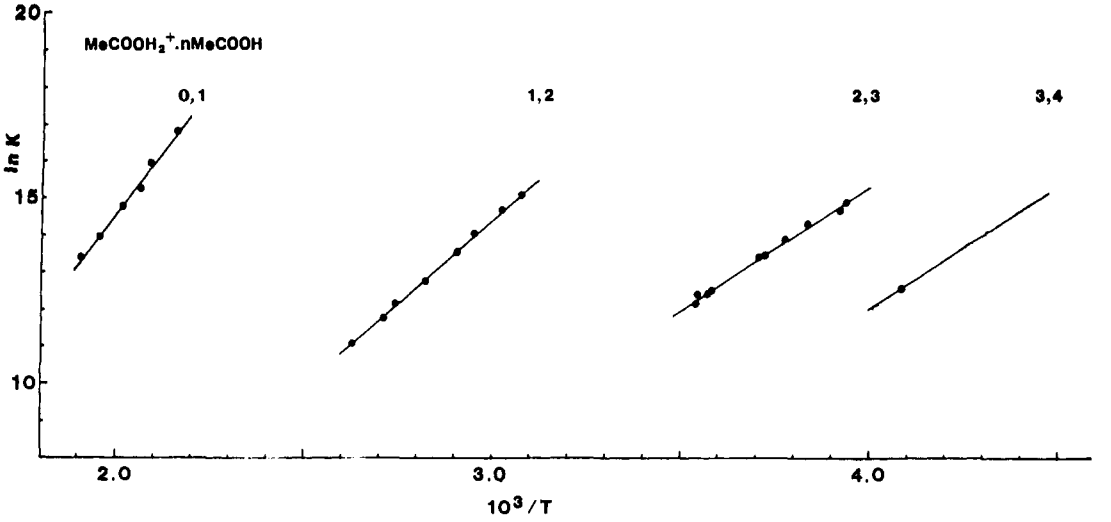

Figure 4. Van't Hoff plots as in Figure 1, for B = MeCOOH. The plot for 3, 4 equilibrium is based on the point shown and estimated $\Delta S°$; see Table I.

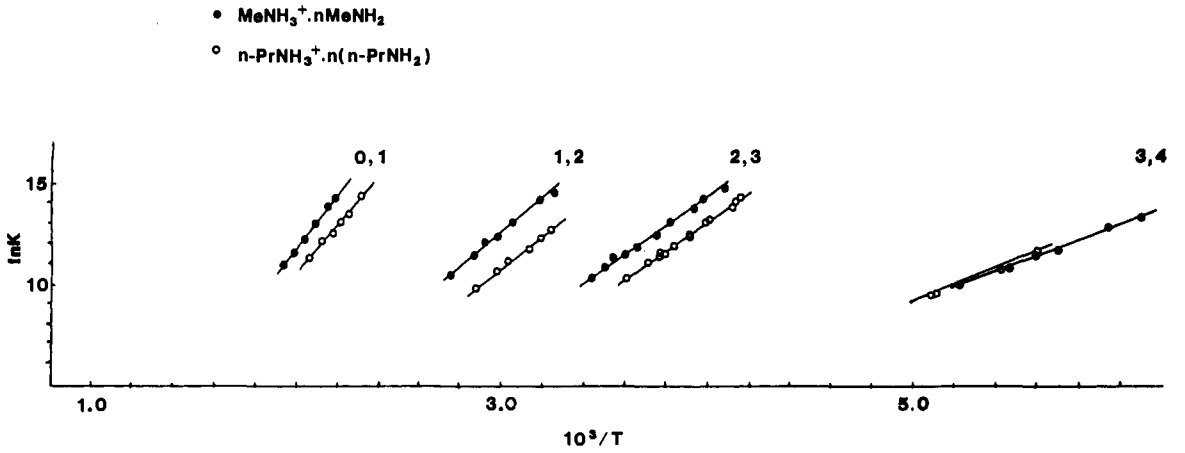

Figure 5. Van't Hoff plots as in Figure 1 for B = $MeNH_2$ and for B = n-$PrNH_2$.

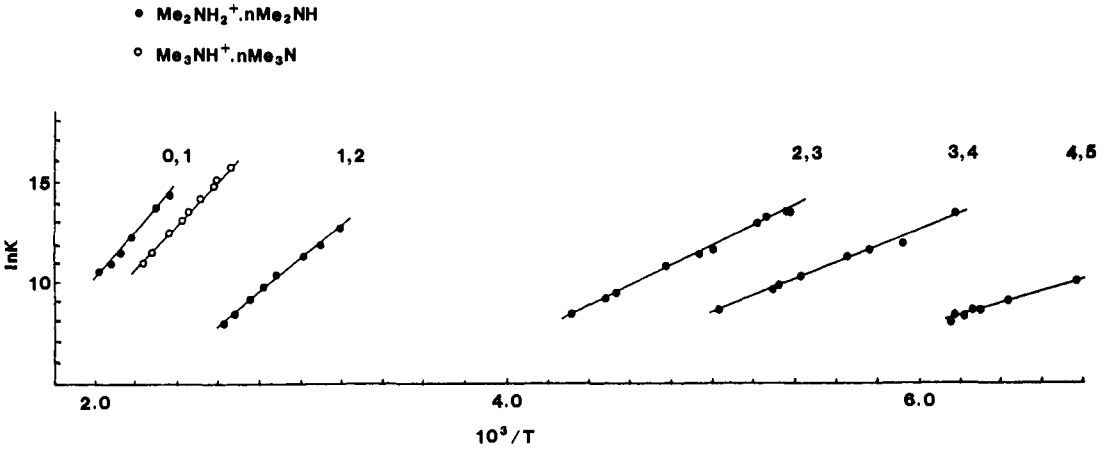

Figure 6. Van't Hoff plots as in Figure 1 for B = Me_2NH and for B = Me_3N.

Because of the limitations on measurements in large clusters, $\Delta G°_{n-1,n}$ for several clusters was measured at a single temperature and $\Delta H°$ was calculated using the estimated $\Delta S°$. This value can be estimated with confidence within ±20 J/(mol K) (±5 cal/(mol K)), since all of the measured $\Delta S°$ for large clusters fall within such a range, and since $-\Delta S°_{n-1,n}$ approaches the known values of $\Delta S°_{evap}$ which can be used for the estimation. These estimations do not necessarily lead to a large uncertainty in $\Delta H°$. For example, at 200 K, the resulting uncertainty in $\Delta H°_{n-1,n}$ is only ±4 kJ/mol (±1 kcal/mol). This is comparable to the error from temperature studies, especially for large clusters that can be measured only over a small range near condensation. Further errors near condensation may result from partial sample condensation and neutral clustering.

Table I compares the present results with literature values. For protonated methanol clusters with n = 3–7, the present values are somewhat smaller than the early results of Grimsrud and Kebarle.[14] The early results could have been affected by decomposition outside the ion source, as was discussed by Sunner et al.[48] and Klots.[49] This was demonstrated, for example, for clusters of $(H_2O)_n^+$ ($n > 4$). The early values[50] for these clusters were too large and were corrected by later studies.[38,51] The present values

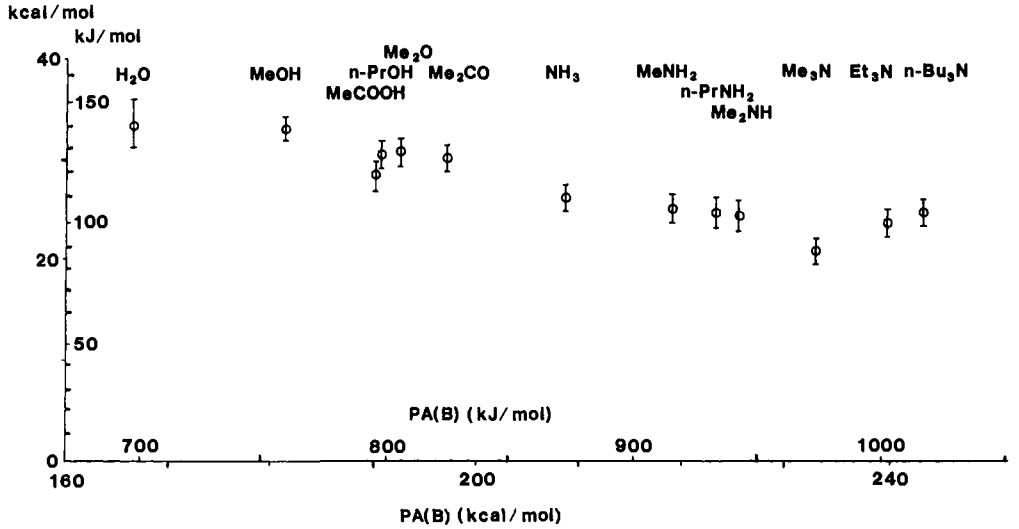

Figure 7. Correlation between $-\Delta H^\circ_{0,1}$, i.e., bonding energies of the dimers B_2H^+, and the proton affinities of the monomers B. Proton affinities below that of NH_3 are from ref 61, and the PA above that of NH_3 are from ref 7. Error bars represent the range of literature data or ±6 kcal/mol, whichever is larger.

apply a similar correction to the early results[14] on the $(MeOH)_nH^+$ clusters ($n > 4$). Thermal cluster decomposition outside the ion source was minimized in the present work by using low partial pressures of MeOH. This allowed measurements at low temperatures. In fact, our highest temperature points for the large clusters were 20–50 K lower than those in the earlier study.[14] In relation to the present results for large alcohol clusters, we also note that the results for $(n\text{-PrOH})_nH^+$, n = 3–5, are in good agreement with Hiraoka et al.[13] (Table I).

In the amine clusters, the present data for $(MeNH_2)_2H^+$ and $(Me_2NH)_2H^+$ differ from literature values[18] (Table I). Our results for $(MeNH_2)_3H^+$ and $(MeNH_2)_4H^+$ also differ from those of Holland and Castleman.[47] We note that the present ΔS° values for these clusters are in the usual range, while the ΔS° values of Holland and Castleman are larger than usual for such clusters. As a check on the present measurements, we redetermined the thermochemistry of $(pyridine)_2H^+$. We found good agreement with our previous results that were obtained using two different mass spectrometers, and with the results of Holland and Castleman on this dimer.[47]

The present data are also supported by internal consistency and by agreement with the usual trends in clustering sequences.[9,40] In the small clusters, the enthalpy sequences, i.e., plots of $-\Delta H^\circ_{n-1,n}$ vs n, show the usual decrease by about a factor of 0.7 in each of the first several steps. The data also show reasonable shell-filling behavior, as discussed below. In the large clusters the present data show the usual trend, i.e., that $-\Delta H^\circ_{n-1,n}$ approaches ΔH_{evap}. These observations suggest that the present data are correct within the stated error limits.

The literature data in Table I are usually consistent if error limits of ±6.3 kJ/mol (±1.5 kcal/mol) in ΔH° and ±17 J/(mol K) (±4 cal/(mol K)) in ΔS° are assigned to data from various sources. Larger inconsistencies may suggest an experimental artifact in one of the data sets. Possible sources of artifacts are discussed in a recent paper.[62]

Discussion

1. Dimer Ions. Hiraoka suggested that the bonding energies of symmetric dimer ions B_2H^+ decrease with increasing proton affinities of the monomers B.[52] In this relation, Table I and Figure 7 show the data for $OH^+\cdot O$ and $NH^+\cdot N$ dimers. The proposed trend is observed, but its magnitude is within the error limits. In the $OH^+\cdot O$ series, $-\Delta H^\circ_{0,1}$ decreases by 13 kJ/mol (3 kcal/mol) over a proton affinity (PA) increase of 130 kJ/mol (32 kcal/mol). In the $NH^+\cdot N$ series from NH_3 to Me_2NH, $-\Delta H^\circ_{0,1}$ decreases by 8 kJ/mol (2 kcal/mol) over a PA increase of 82 kJ/mol (20 kcal/mol). In both series, the slope of $\Delta H^\circ_{0,1}$ vs PA is about 0.1. In fact, the two series fit one combined correlation line over a range of 38 kJ/mol (9 kcal/mol) in $-\Delta H^\circ_{0,1}$ and of 250 kJ/mol (60 kcal/mol) in PA(B).

Deviations from the correlation line are small and within the error limits, but they may have structural meaning. The hydrogen bond strength in $(MeCOOH)_2H^+$ may be slightly decreased because of resonance charge delocalization in the monomer ion $MeC(OH)_2^+$ which decreases the charge on the hydrogen-bonding proton. The hydrogen bond between the nitrogen centers in $(Me_3N)_2H^+$ may be slightly weakened by steric crowding. However, the interaction energy in the even more crowded $(Et_3N)_2H^+$ and $(n\text{-}Bu_3N)_2H^+$ increases again. This may be due to attractive dispersive interactions, i.e., hydrophobic bonding, between the alkyl groups of the component molecules.

Except for these highly crowded species, in dimer ions the alkyl groups do not appear to interact significantly with the charge centers or with each other.

2. Hydrogen Bonding to Core Ions. Enthalpy sequences of $-\Delta H^\circ_{n-1,n}$ vs n are shown in Table I. The bonding energy of the nth neutral molecule to the core ion is remarkably constant irrespective of alkylation. The preceding section showed that $-\Delta H^\circ_{0,1}$ varies only slightly, in correlation with the proton affinities. As to the further ligand molecules in the inner shell, the value of $-\Delta H^\circ_{1,2}$ is constant at 88 ± 4 kJ/mol (21 ± 1 kcal/mol) in the $OH^+\cdot O$ clusters and at 67 ± 4 kJ/mol (16 ± 1 kcal/mol) in the $NH^+\cdot N$ clusters. Further, for inner shell ligands, $-\Delta H^\circ_{2,3}$ is 58 ± 4 kJ/mol (14 ± 1 kcal/mol) and $-\Delta H^\circ_{3,4}$ is 12 ± 4 kJ/mol (12 ± 1 kcal/mol) in both sets. The only series that differs slightly from these constant values are the MeCOOH clusters where the bonding energy in each step is weakened by 4–8 kJ/mol (1–2 kcal/mol) compared with the alcohols, possibly due to resonance effects.

These results therefore show that the bonding energies to the core ions are not affected by alkyl substitution. If hydrophobic interactions did occur, they could increase the bonding energies but would also cause significant entropy loss. The absence of such effects suggests that the inner shell ligands are purely hydrogen bonded to the core ions, and the alkyl groups are oriented away from the hydrogen-bonding centers and also do not interact with each other. This is illustrated schematically by conformation 1. The opposite extreme would be the schematic conformation 2, where the alkyl groups would interact and make a stabilizing contribution. Of course, mixed conformations are also possible. It is possible that conformations with stabilizing hydrophobic interactions will predominate at low temperatures where the entropy effects are not significant, such as in supersonic beam expansion.

3. Shell Effects. The solid lines in Figure 8 show $-\Delta H^\circ_{n-1,n}$ for the $RNH_3^+\cdot nRNH_2$ and $H_3O^+\cdot nH_2O$ sequences. In both, the

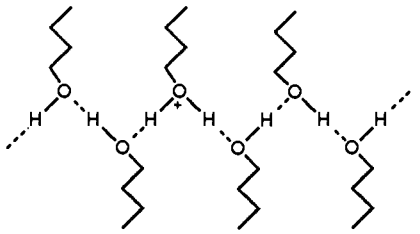

1

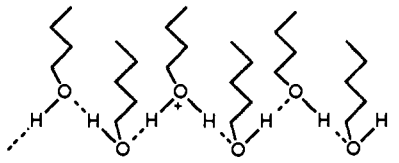

2

core ions have three protic hydrogens available for hydrogen bonding. Correspondingly, a significant drop is observed in $-\Delta H°_{n-1,n}$ after filling the first shell, i.e., at the 3, 4 step. An effect of similar magnitude is observed in Figure 8 in the $NH_4^+ \cdot nNH_3$ sequence after filling the first shell, i.e., at the 4, 5 step, and in Figure 9 in the $Me_2NH_2^+ \cdot nMe_2NH$ sequence at the 2, 3 step. The shell effects are also evident in the spacing of van't Hoff plots in Figures 5 and 6.

A quantitative value can be assigned to the shell effect in $RNH_3^+ \cdot nRNH_2$ by estimating a hypothetical $-\Delta H°_{3,4}$ value in the absence of the shell effect, i.e., the value that would obtain if the decrease in $-\Delta H°_{n-1,n}$ was smooth. This can be done by extrapolating from the preceding steps, or by using the $NH_4^+ \cdot nNH_3$ sequence as a model where shell filling does not occur at the 3, 4 step. Both estimates give a hypothetical value of about 50 kJ/mol (12 kcal/mol) for $-\Delta H°_{3,4}$ in the $RNH_3^+ \cdot nRNH_2$ clusters, compared with the actual values of 32 kJ/mol (7 kcal/mol) in the $MeNH_3^+ \cdot nMeNH_2$ and the $n\text{-}PrNH_3^+ \cdot n\text{-}PrNH_2$ sequences. The difference suggests that shell filling results in a drop of 18 kJ/mol (4.5 kcal/mol) in $-\Delta H°_{n-1,n}$. Analogous extrapolations show a drop of 12–16 kJ/mol (3–4 kcal/mol) in the $NH_4^+ \cdot nNH_3$ sequence after the 3, 4 step and of 21 kJ/mol (5 kcal/mol) in $H_3O^+ \cdot nH_2O$ after the 2, 3 step.

Figure 9 shows the $-\Delta H°_{n-1,n}$ sequences for clusters where the core ions have two hydrogen-bonding sites, i.e., $Me_2NH_2^+ \cdot nMe_2NH$, $MeOH_2^+ \cdot nMeOH$, and $n\text{-}PrOH_2^+ \cdot n(n\text{-}PrOH)$. Here shell filling should cause a drop in $-\Delta H°_{n-1,n}$ at the 2, 3 step. No obvious drop is observed, but a knee at the 1, 2 step is followed by a drop at the 2, 3 step. Comparison can be made with the $H_3O^+ \cdot nH_2O$ and $MeNH_3^+ \cdot MeNH_2$ sequences, where there is no shell filling at the 2, 3 step (see dotted lines in Figure 9). Using this comparison, a shell-filling effect of about 12 kJ/mol (3 kcal/mol) at the 1, 2 step becomes apparent also in the alcohol series.

These considerations show that the magnitude of the shell effect is not affected by the degree of alkyl substitution at the core ion. This is somewhat unexpected, since the effect reflects the differences between the charge densities on the hydrogen-bonding atoms in the inner and outer shells. This difference should decrease as alkyl substituents decrease the charge densities at the core ion itself.

The observed effect may be explained as follows. From protonated ammonia to primary and secondary amines, more charge is delocalized to the alkyl substituents. On the other hand, in the same series, shell filling occurs at earlier steps, when less neutral molecules are present in the clusters. The two effects, intramolecular charge delocalization to alkyl groups and intermolecular charge delocalization to ligand molecules, therefore vary in opposite directions with alkylation, and may cancel. Similar arguments may apply in comparing water clusters to alcohol clusters.

A very large shell-filling effect is observed in the blocked dimer $(Me_3N)_2H^+$. Since there are no further conventional hydrogen-bonding sites available, $-\Delta H°_{n-1,n}$ shows a large drop in going to

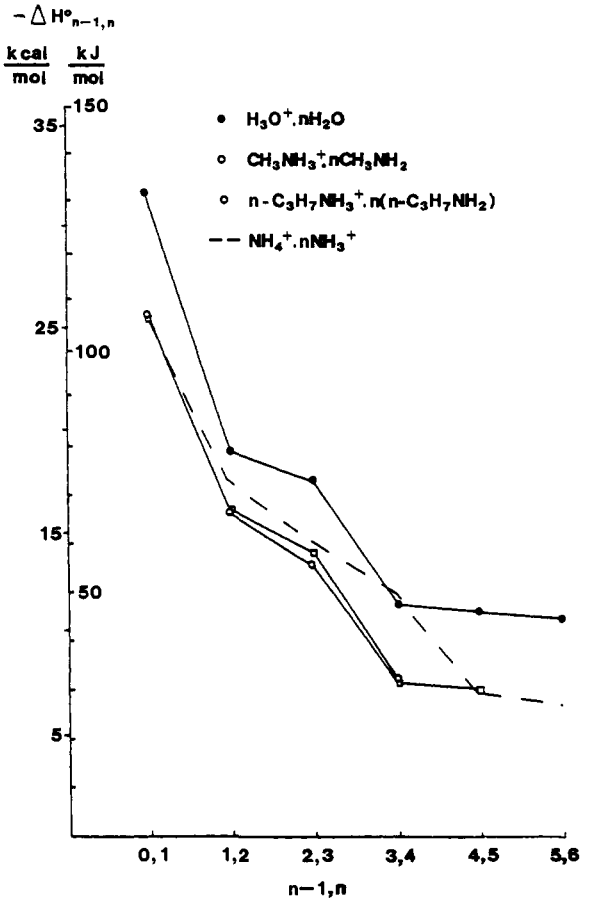

Figure 8. Enthalpy sequences ($-\Delta H°_{n-1,n}$ vs n) for clusters about core ions with three hydrogens: (●) $H_3O^+ \cdot nH_2O$; (○) $MeNH_3^+ \cdot nMeNH_2$; (□) $n\text{-}PrNH_3^+ \cdot n\text{-}PrNH_2$. For comparison, the sequence for $NH_4^+ \cdot nNH_3$, where shell filling does not occur at the 3, 4 step, is shown by the broken line.

$(Me_3N)_3H^+$ (Table I), in analogy with the behavior in the Me_2O, Me_2CO, and MeCN clusters.[14,16,53] These results are in agreement with the recent $(Me_3N)_nH^+$ results of Wei et al.[58]

Table I shows a consistent trend also in the entropies. For all the clusters, $-\Delta S°_{0,1}$ is 118 ± 4 J/(mol K) (28 ± 1 cal/(mol K)) and $-\Delta S°_{1,2}$ is 108 ± 8 J/(mol K) (26 ± 1 cal/(mol K)). As to shell effects, in all of the entropy sequences in Table I there is a decrease by 16–25 J/(mol K) (4–6 cal/(mol K)) in $-\Delta S°_{n-1,n}$ on going from the filled inner shell to the looser outer shell. The effect is most convincing in $(H_2O)_nH^+$ and $(NH_3)_nH^+$, where the data are average values from several laboratories.[9]

4. The Outer Shells. This section will examine the experimental bonding energies in the outer shells of the $(ROH)_nH^+$ clusters, and compare them with other clustering sequences.

The alcohol clusters are interesting since the hydrogen-bonded network is a chain, and each molecule can attach by only one OH···O bond. If a structure like 1 extended indefinitely, the limiting value of $-\Delta H°_{n-1,n}$ in large clusters should approach the strength of a neutral OH···O bond, 20 kJ/mol (5 kcal/mol). To examine this, we extended the $(MeOH)_nH^+$ series to $n = 14$ (see Table I, footnote *b*, and Figure 9). The limiting value is 34 ± 4 kJ/mol (8 ± 1 kcal/mol), which is larger by 12 kJ/mol (3 kcal/mol) than the strength of a single OH···O bond. In fact, $-\Delta H°_{n-1,n}$ approaches the bulk condensation energy, which includes contributions from interactions of the methyl groups.

Similar trends are seen in the experimental $-\Delta H°_{n-1,n}$ in $(n\text{-}PrOH)_nH^+$ and $(n\text{-}AmOH)_nH^+$, which again approach $\Delta H°_{evap}$ of about 46 kJ/mol (11 kcal/mol); see Table I and Figure 9. This suggests (with the reservations discussed below) contribution of about 25 kJ/mol (6 kcal/mol) by the longer alkyl chains. (Note that the enthalpy series are limited, especially in *n*-AmOH, because of sample condensation.) Similar trends are observed also in the

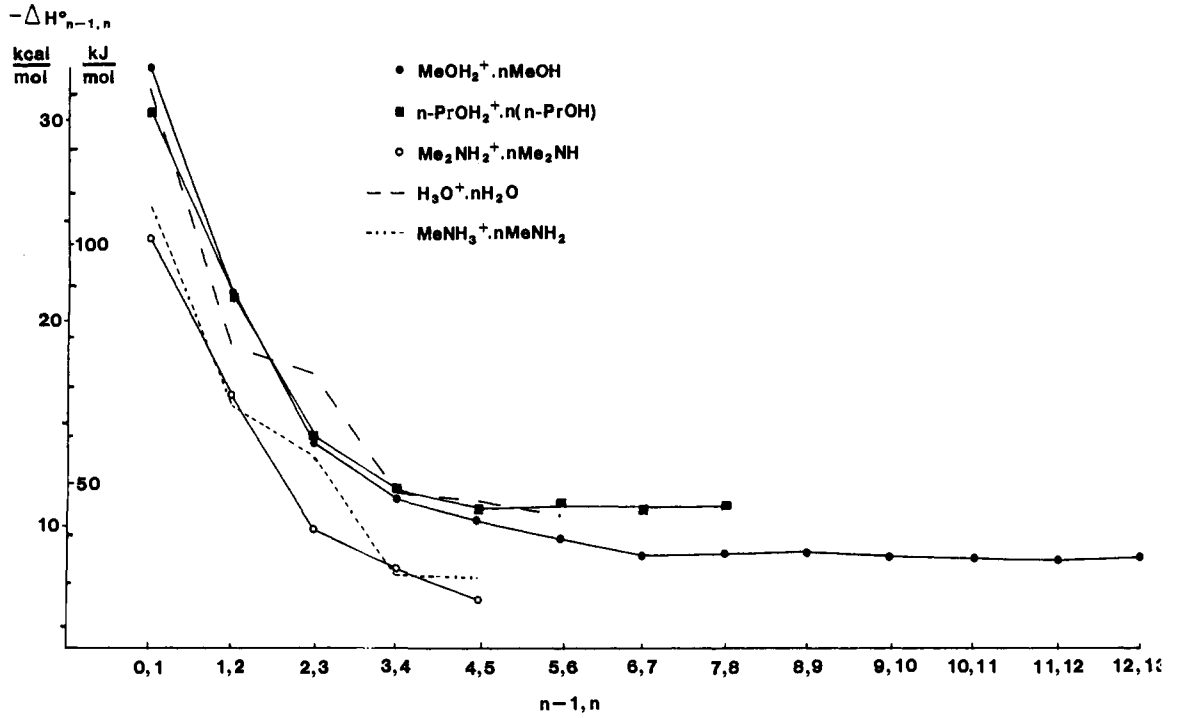

Figure 9. Enthalpy sequences for clusters about core ions with two hydrogens: (●) $MeOH_2^+ \cdot n$MeOH; (■) n-$PrNH_2^+ \cdot n$PrOH; (○) $Me_2NH_2^+ \cdot n Me_2NH$. For comparison, the sequences for $H_3O^+ \cdot nH_2O$ (broken line) and for $MeNH_3^+ \cdot n MeNH_2$ (dotted line), where shell filling does not occur at the 2, 3 step, are also shown.

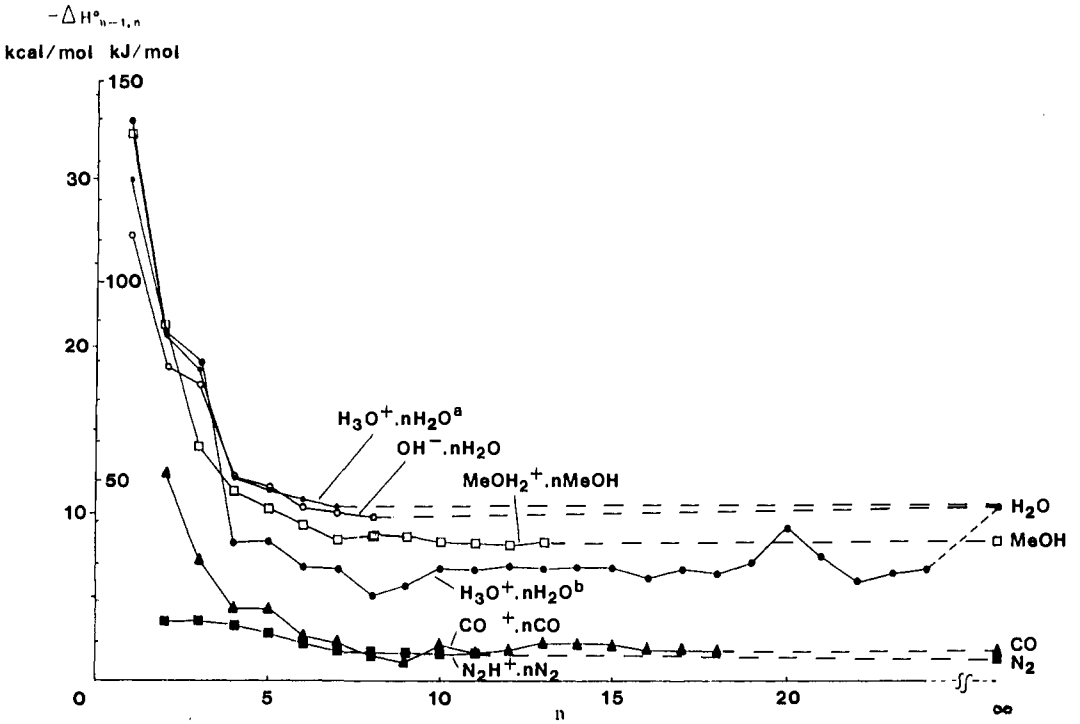

Figure 10. Relation between $\Delta H°_{n-1,n}$ and $\Delta H°_{evap}$ in the enthalpy series shown: (a) from the average of literature equilibrium values in ref 9; (b) CID results from ref 66. Other data are from the references quoted in Table II.

MeOH and *n*-PrOH clusters about ROH_2^+ or Cl^- core ions, which reach the same limiting values despite the very different interactions in the inner shells[42] (Table II). The results suggest (again, with the reservations discussed below) alkyl chain interactions as in the schematic structure 2 above. At the experimental tem-

(22) Hiraoka, K. *J. Chem. Phys.* **1987**, *87*, 4048.
(23) Hiraoka, K.; Mori, T. *J. Chem. Phys.* **1989**, *90*, 7143.
(24) Hiraoka, K.; Nakajima, G.; Shoda, S. *Chem. Phys. Lett.* **1988**, *146*, 535.
(25) Hiraoka, K.; Mizuse, S.; Yamabe, S. *J. Chem. Phys.* **1987**, *87*, 3647.
(26) Hiraoka, K. *J. Chem. Phys.* **1988**, *89*, 3190.
(27) Hiraoka, K. *Chem. Phys.* **1988**, *125*, 439.
(28) Hiraoka, K.; Nakajima, G. *J. Chem. Phys.* **1988**, *88*, 7709.
(29) Hiraoka, K.; Yamabe, S. *Chem. Phys. Lett.* **1989**, *154*, 139.
(30) Hiraoka, K.; Yamabe, S. *J. Chem. Phys.* **1989**, *90*, 3268.
(31) Hiraoka, K.; Kebarle, P. *Can. J. Chem.* **1977**, *55*, 24.
(32) Castleman, A. W.; Holland, P. M.; Lindsay, D. M.; Peterson, K. I. *J. Am. Chem. Soc.* **1978**, *100*, 6039.
(33) Arshadi, M. R.; Futrell, J. H. *J. Phys. Chem.* **1974**, *78*, 1482.
(34) Hiraoka, K.; Kebarle, P. *J. Am. Chem. Soc.* **1975**, *97*, 4179.

Table I. Thermochemistry[a] of Clustering Reactions $BH^+\cdot(n-1)B + B \rightarrow BH^+\cdot nB$

B	$n-1, n$	$-\Delta H°_{n-1,n}$ kJ/mol	$-\Delta H°_{n-1,n}$ kcal/mol	$-\Delta S°_{n-1,n}$ J/(mol K)	$-\Delta S°_{n-1,n}$ cal/(mol K)
H_2O	0, 1	*140*	*33.5*	*122*	*29.1*
	1, 2	*87*	*20.8*	*109*	*26.0*
	2, 3	*73*	*17.4*	*116*	*27.8*
	3, 4	*51*	*12.3*	*93*	*22.2*
	4, 5	*49*	*11.8*	*99*	*23.6*
	5, 6	*44*	*10.7*	*109*	*26.1*
MeOH	0, 1	136, 138[c]	32.6, 33.1[c]	121, 128[c]	29.0, 30.5[c]
		134,[d] *137*	32.1,[d] *32.6*	111,[d] *120*	26.6,[d] *28.7*
	1, 2	89,[b] 89[c]	21.2,[b] 21.3[c]	113,[b] 118[c]	27.0,[b] 28.2[c]
		88,[d] *89*	21.0,[d] *21.2*	108,[d] *113*	25.8,[d] *27.0*
	2, 3	59,[b] 67[c]	14.0,[b] 16.1[c]	100,[b] 121[c]	24.0,[b] 28.9[c]
	3, 4	47,[b] 56[c]	11.3,[b] 13.5[c]	93,[b] 120[c]	22.3,[b] 28.7[c]
	4, 5	43,[b] 52[c]	10.2,[b] 12.5[c]	99,[b] 130[c]	23.5,[b] 31.1[c]
	5, 6	39,[b] 50[c]	9.3,[b] 11.9[c]	97,[b] 138[c]	23.5,[b] 32.9[c]
	6, 7	38,[b] 50[c]	9.0,[b] 12.0[c]	108,[b] 149[c]	25.7,[b] 35.7[c]
	7, 8	39[b]	9.4[b]	93[b]	26.9[b]
	8, 9	38[b,e]	9.1[b,e]	(109)	(26)
	9, 10	36[b,e]	8.7[b,e]	(109)	(26)
	10, 11	36[b,e]	8.6[b,e]	(109)	(26)
	11, 12	36[b,e]	8.5[b,e]	(109)	(26)
	12, 13	34[b,e]	8.2[b,e]	(109)	(26)
n-PrOH	0, 1	127[f]	30.4[f]	112[f]	26.7[f]
	1, 2	90, 79[g]	21.6, 18.9[g]	131, 96[g]	31.4, 23.0[g]
	2, 3	60, 59[g]	14.4, 14.2[g]	107, 100[g]	25.5, 23.8[g]
	3, 4	50, 49[g]	11.9, 11.7[g]	104, 96[g]	24.8, 23.0[g]
	4, 5	46	10.9	106	25.4
	5, 6	46	11.1	120	28.8
	6, 7	46	10.9	128	30.5
	7, 8	46[h]	11[h]	(125)	(30)
n-AmOH	1, 2	92[h]	22[h]	(105)	(32)
	2, 3	59	14.0	102	24.3
	3, 4	50	11.9	94	24.4
	4, 5	46[h]	11[h]	(105)	(25)
MeCOOH	0, 1	118	28.1	118	28.3
	1, 2	77	18.5	102	24.5
	2, 3	55	13.1	94	22.4
	3, 4	50[h]	12[h]	(105)	(25)
$(Me)_2O$	0, 1	128,[i] 123[j]	30.7,[i] 29.5[j]	124,[i] 113[j]	29.6,[i] 27.0[j]
		134,[k] *128*	32.0,[k] *30.7*	133,[k] *123*	31.9,[k] *29.5*
	1, 2	42[i]	10.1[i]	115[i]	23.0[i]
Me_2CO	0, 1	126,[l] 128[k]	30.1,[i] 30.7[k]	127,[l] 118[k]	30.4,[l] 28.2[k]
		124,[m] *126*	29.6,[m] *30.1*	123,[m] *123*	29.3,[m] *29.3*
	1, 2	60[l]	12.2[i]	96[l]	23.0[i]
NH_3	0, 1	*109*	*26.0*	*117*	*27.9*
	1, 2	*69*	*16.6*	*102*	*24.4*
	2, 3	*57*	*13.7*	*105*	*25.1*
	3, 4	*49*	*11.7*	*110*	*26.4*
	4, 5	*29*	*7.0*	*90*	*21.5*
	5, 6	*27*	*6.5*	*92*	*21.9*
$MeNH_2$	0, 1	106, 91[n]	25.4, 21.7[n]	114, 99[n]	27.3, 23.6[n]
	1, 2	67, 80[o]	16.0, 19.2[o]	96, 167[o]	22.9, 39.9[o]
	2, 3	56, 71[o]	13.4, 17.0[o]	105, 174[o]	25.1, 41.6[o]
	3, 4	33	7.8	90	21.5
n-$PrNH_2$	0, 1	102	24.5	115	27.6
	1, 2	67, 82[o]	16.0, 19.5[o]	110, 174[o]	26.3, 41.6[o]
	2, 3	59, 72[o]	14.0, 17.1[o]	126, 177[o]	30.1, 42.3[o]
	3, 4	32	7.7	84	20.1
	4, 5	29	7	(92)	(22)
Me_2NH	0, 1	101, 87[n]	24.1, 20.8[n]	118, 108[n]	28.1, 25.7[n]
	1, 2	69	16.4	174	27.2
	2, 3	41	9.9	109	26.1
	3, 4	33	7.9	94	22.5
	4, 5	26	6.3	94	22.5
Me_3N	0, 1	92, 94[n]	22.0, 22.5[n]	114, 134[n]	27.2, 32.0[n]
		100[p]	24[p]		
	1, 2	<33, 29[p]	<8, 6.9[p]		
pyridine	0, 1	105, 103[q]	25.2, 24.6[q]	124, 118[q]	29.6, 28.2[q]
		99,[r] 110[o]	23.7,[r] 26.3[o]	117,[r] 134[o]	28.0,[r] 32.1[o]

[a] Values from this work unless noted otherwise. Values in italics are average of selected tabulated values from ref 9 or average of three or more data sets listed here. Values in parentheses are estimated. [b] Reference 10. [c] Reference 11. [d] Reference 12. [e] For higher steps in $(MeOH)_nH^+$, the entropy change is assumed as shown, and $-\Delta H°_{n-1,n}$ is calculated from single-temperature measurements of $-\Delta G°$ (kJ/mol (kcal/mol), T): (8, 9), 16, (3.9), 200; (9, 10) 15, (3.5), 200; (10, 11) 16, (3.8), 184; (11, 12) 16, (3.7), 184; (12, 13) 16, (3.8), 184. [f] Present work, from thermochemical cycles involving the following switching reactions and $\Delta H°$ and $\Delta S°$ values: $(MeCN)_2H^+ + n\text{-PrOH} \rightarrow n\text{-}PrOH_2^+\cdot MeCN + MeCN$, −13 (−3.1), −2 (−0.5); $n\text{-}PrOH_2^+\cdot MeCN + n\text{-PrOH} \rightarrow (n\text{-PrOH})_2^+ + MeCN$, +0.4 (+0.1), −6 (−1.4); also $MeCNH^+ + MeCN \rightarrow (MeCN)_2H^+$, −125 (−29.8), −104 (−24.8) from ref 57. [g] Reference 13. [h] Calculated using assumed $-\Delta S°_{n-1,n}$ values as shown, and experimental $-\Delta G°_{n-1,n}(T)$ values as follows.

(footnotes to Table I continued)

n-PrOH: (8, 9) 17, (4.1), 215. *n*-AmOH: (1, 2) 44, (10.5), 346; (4, 5) 21, (5.1), 227. MeCOOH: (3, 4) 26, (6.2), 245. *n*-$PrNH_2$: (4, 5) 14, (3.4), 174. Me_3N: (1, 2) <17, (<4.0), 195. [i] Reference 14. [j] Reference 15. [k] Reference 7. [l] Reference 16. [m] Reference 17. [n] Reference 18. [o] Reference 19. [p] Reference 58. [q] Reference 20. [r] Reference 21.

Table II. Limiting Enthalpies[a] for the Condensation of Neutral Molecules on Large Clusters and Condensation Enthalpies of the Macroscopic Liquids[b]

neutral	ion	$-\Delta H°_{lim}$ (kJ/mol)	$\Delta H°_{vap}$ (kJ/mol)	$-\Delta H°_{lim}$ (kcal/mol)	$\Delta H°_{vap}$ (kcal/mol)	n[c]	ref
H_2	H_3^+	2.5	0.8	0.6	0.2	9	22
Ar	Ar^+	6.2		1.5		10	23
N_2	N_2^+	7.1	5.4	1.7	1.3	11	29
	N_3^+	5.9	5.4	1.4	1.3	11	29
	O_2^+	5.9	5.4	1.4	1.3	11	29
	NO_2^+	6.3	5.4	1.5	1.3	12	30
	NO^+	7.1	5.4	1.7	1.3	10	30
	N_2H^+	7.1	5.4	1.7	1.3	11	69
	O_3	6.3	5.4	1.5	1.3	9	27
	O_4^-	6.7	5.4	1.6	1.3	8	27
CO	CO^+	7.5	6.0	1.8	1.4	18	67
	CO_2H^+	7.5	6.0	1.8	1.4	14	69
O_2	O_2^+	7.5	6.7	1.8	1.6	8	26
	O_2^+	7.1	6.7	1.7	1.6	9	67
	O_2^-	5.9	6.7	1.4	1.6	8	26
	O_3^-	6.3	6.7	1.5	1.6	5	27
CH_4	CH_5^+	17	8.4	4	2.0	4	34
CO_2	CO_2^+	17	17	4	4	6	24
	O_2^+	17	17	4	4	6	24
	F^-	21	17	5	4	5	25
	I^-	17	17	4	4	4	25
H_2S	H_3S^+	25	19	6	4.5	4	31
NH_3	Na^+	38	23	9	5.6	6	32
	NH_4^+	29	23	7	5.6	6	33
	NH_4^+	17	23	4	5.6	17	70
H_2O	Na^+	46	44	11	10.5	6	35
	K^+	42	44	10	10.5	6	36
	H_3O^+	46	44	11	10.5	6	37
		46	44	11	10.5	6	38
		32	44	8	10.5	27	66
	$MeOH_2^+$	38	44	9	10.5	6	39
		38	44	9	10.5	6	40
	$EtOH_2^+$	42	44	10	10.5	5	39
	n-$PrOH_2^+$	38	44	9	10.5	6	39
	i-$PrOH_2^+$	38	44	9	10.5	6	39
	n-$PrNH_3^+$	42	44	10	10.5	4	40
	OH^-	42	44	10	10.5	7	38
	F^-	46	44	11	10.5	9	41
	Cl^-	38	44	9	10.5	9	41
	Br^-	42	44	10	10.5	6	41
	I^-	38	44	9	10.5	4	41
	H_2COH^+	42	44	10	10.5	7	40
	$MeCHOH^+$	42	44	10	10.5	6	40
	$(Me)_2COH^+$	42	44	10	10.5	5	40
MeOH	$MeOH_2^+$	34	35	8	8.4	14	
	$CH_3OCH_2CH_2OCH_3H^+$	34	35	8	8.4	6	43
	Cl	17	35	7	8.4	10	42
EtOH	Cl^-	38	42	9	10.1	8	42
i-PrOH	Cl^-	46	46	11	10.9	7	42
n-PrOH	*n*-$PrOH_2^+$	46	41	11	9.9	7	
	Cl^-	46	41	11	9.9	7	42
t-BuOH	Cl^-	46	(50)	11	(12)	5	42
n-AmOH	*n*-$AmOH_2^+$	46	56	11	13.4	4	
MeCOOH	$MeCOOH_2^+$	50	54	12	12.8	4	
HCN	NH_4^+	29	25	7	6.0	6	43
	CN^-	29	25	7	6.0	7	44
	I^-	29	25	7	6.0	8	44
MeCN	$MeCNH^+$	29	33	7	7.9	4	43
	F^-	38	33	9	7.9	7	41
	Cl^-	38	33	9	7.9	7	41
	Br^-	33	33	8	7.9	7	41
	I^-	29	33	7	7.9	5	41
Me_3N	Me_3NH^+	29	23	7	5.5	7	58
Me_2SO	K^+	63		15		6	45
	Cl^-	59		14		5	46

[a] $\Delta H°$ in kcal/mol, $\Delta S°$ in cal/mol K. Limiting values correspond to $-\Delta H°_{n,n+1}$ and $-\Delta S°_{n,n+1}$ for the largest n measured, or extrapolated from the variation with n. [b] From ref 56 or 63. Values in parentheses are estimated from homologous series. [c] The largest n for which thermochemistry was measured.

peratures, the structure probably fluctuates between many isomeric conformations of similar energy. In fact, ab initio studies show that, with increasing cluster size, the number of conformational isomers of similar energies also increases rapidly.[55]

From the limited data for $(MeCOOH)_nH^+$, the value of $-\Delta H°_{n-1,n}$ appears to approach about 50 kJ/mol (12 kcal/mol), similar to $\Delta H°_{evap}$. This value reflects contributions by the large dipole moment of MeCOOH.

The literature enthalpy sequences in alcohols and other molecules are summarized and compared with the bulk $\Delta H°_{evap}$ in Figure 10 and Table II. Most clustering sequences extend to n = 4–10, with some studies[67] up to n = 18 and a recent collisional dissociation study up to n = 28.[66] In all the equilibrium studies, the $-\Delta H°_{n-1,n}$ values decrease asymptotically toward $\Delta H°_{evap}$, and reach this value within the usual experimental accuracy of ±6 kJ/mol (±1.5 kcal/mol) usually at n = 6–10. (Note that the appropriate values of ΔH_{evap} for these comparisons would be the values at the pressures and temperatures where the limits of the clustering series are measured, and should also be corrected for cluster size. However, since these values are generally not available, the values are given under standard temperature and pressure (STP) conditions or at the boiling points of liquids.)

The data show near coincidence of $-\Delta H°_{n-1,n}$ (n = 6–10) with $\Delta H°_{evap}$. This applies to small molecules with very low $\Delta H°_{evap}$, such as H_2, N_2, and CO, polar molecules such as MeCN, and hydrogen bonding liquids such as H_2O and alcohols (Table II). This coincidence suggests liquidlike structures and interactions in these small clusters, even though most of the molecules are on the surface. The bulklike thermochemistry is surprising for the following reasons.

A theoretical model for the attachment energies is based on the continuum model of the Thomson equation (eq 1),[64] where M is the molecular weight, ρ the density, σ the surface tension, and e the dielectric constant of the bulk solvent. On the RHS

$$\Delta G_{n-1,n} = RT \ln p° + A(M_2/\rho^2 n)^{1/3}\sigma - B(1 - e^{-1})n^{-4/3}(\rho/M)^{1/3} \quad (1)$$

of eq 1, $p°$ is the equilibrium vapor pressure of the bulk solvent, and the other two terms are size-dependent corrections due to surface tension (unsaturated surface forces) and dielectric charging energy. The value of $\Delta S°$ is found from the temperature derivative and that of $\Delta H°$ from $\Delta G° + T\Delta S°$. Note that the negative dielectric energy varies more steeply with n than the positive surface energy. The calculated $-\Delta H°_{n-1,n}$ therefore undershoots the limiting macroscopic condensation energy (although not substantially) and then slowly approaches it at large n, as discussed by Holland and Castleman.[64] Indeed, the calculated Thomson plots of $\Delta H°_{n-1,n}$ show small minima of 4–8 kJ/mol (1–2 kcal/mol) at n = 10–15.[64]

Only a few of the experimental sequences extend to this size, and the accuracies are not sufficient to test the predicted small undershoot. It is consistent with the Thomson equation that the measured limiting $-\Delta H°_{n-1,n}$ values should not be very different, within the usual experimental error of ±1 kcal/mol, from the bulk $\Delta H°_{evap}$ already at about n = 6–10, although this is due to a coincidence of canceling terms.

In terms of the contributing physical factors, this may be due to the small values of the size-dependent surface tension and dielectric terms at $n > 10$. For example, the enthalpy derived from eq 1 for hydrated clusters $BH^+ \cdot nH_2O$ gives $\Delta H°_{n-1,n}$(cavity) and $\Delta H°_{n-1,n}$(dielectric) as 10.0 kJ/mol (2.4 kcal/mol) and −5.7 kJ/mol (−1.4 kcal/mol), respectively, at n = 10. These terms depend on the continuum model used. The limitations of these models were discussed by, among many others, Holland and Castleman[64] and Meot-Ner.[1]

As the surface and dielectric terms are of opposite sign, a coincident cancelation may occur in all the clusters in Table II. However, these terms depend on molecular parameters (ρ, σ, and e) that vary independently among the molecules in Table II. Therefore, the universal coincidence of $-\Delta H°_{n-1,n}$ with $\Delta H°_{evap}$ is unlikely to be coincidental. It suggests liquidlike structures and interactions already in n = 6–10 clusters, and a near cancelation of the small cavity and dielectric terms at these cluster sizes.

Ab initio charge densities also suggest that the dielectric charge effects may be small already in small clusters. For example, 6-31G* Mulliken atomic charges are 0.488 on the protons of NH_4^+, but only 0.373 on the outer protons already in $NH_4^+ \cdot 3NH_3$, and 0.355 on NH_3 molecules in the second shell.[55] These outer shell protons have atomic charges near that of 0.332 of neutral NH_3.[55] Also, in the outer shells theoretical models[65] and experiments[58-60] suggest cyclic structures, and the net number of hydrogen bonds may approach the bulk value. The molecular models therefore also suggest that the size-dependent correction terms in eq 1 may be small already in modest size clusters, even though most molecules are on the surface.

Taking the experimental coincidence of $-\Delta H°_{n-1,n}$ and $\Delta H°_{evap}$ at face value, or assuming compensating surface and dielectric forces, both allow us to assign 12–25 kJ/mol (3–6 kcal/mol) to the hydrophobic alkyl–alkyl interactions in the outer shells of the alcohol clusters. Such interactions would be consistent with the observation by Castleman et al. that "At larger sizes...the ligand molecules can begin to interact sterically with each other...As the enthalpy of reaction begins to approach the heat of condensation, ligand–ligand interactions can become more important...Here a well-defined structure becomes less meaningful...".[54] The present results extend this to complex alkylated molecules.

In relation to the present $(ROH)_nH^+$ series, a recent study of Magnera et al.[66] on the first 28 $(H_2O)_nH^+$ binding energies is very interesting. The results show a possible minimum at n = 9, where $E_{n-1,n}$ = 5.5 ± 1 kcal/mol, and a slow rise to about 7 ± 1 kcal/mol at n = 26, which is still significantly smaller than $\Delta H°_{evap}$. The significant undershoot is attributed to numerous dangling hydrogen bonds in the $(H_2O)_nH^+$ clusters.[66] In contrast, $(ROH)_nH^+$ clusters of any size can have at most two dangling bonds, and they should show much smaller undershoot. The present results are consistent

(35) Dzidic, I.; Kebarle, P. *J. Phys. Chem.* **1970**, *74*, 1466.
(36) Searles, S. K.; Kebarle, P. *Can. J. Chem.* **1969**, *47*, 2619.
(37) Lau, Y. K.; Ikuta, S.; Kebarle, P. *J. Am. Chem. Soc.* **1982**, *104*, 1462.
(38) Meot-Ner (Mautner), M.; Speller, C. V. *J. Phys. Chem.* **1986**, *90*, 6616.
(39) Hiraoka, K.; Takimoto, H.; Morise, K. *J. Am. Chem. Soc.* **1986**, *108*, 5863.
(40) Meot-Ner (Mautner), M. *J. Am. Chem. Soc.* **1984**, *106*, 1265.
(41) Hiraoka, K.; Mizuse, S.; Yamabe, S. *J. Phys. Chem.* **1988**, *92*, 3943.
(42) Hiraoka, K.; Mizuse, S. *Chem. Phys.* **1987**, *118*, 457.
(43) Meot-Ner (Mautner), M. Unpublished results.
(44) Meot-Ner (Mautner), M.; Cybulsky, S. M.; Scheiner, S.; Liebman, J. F. *J. Phys. Chem.* **1988**, *92*, 2738.
(45) Sunner, J.; Kebarle, P. *J. Am. Chem. Soc.* **1984**, *106*, 6135.
(46) Magnera, T. F.; Caldwell, G.; Sunner, J.; Ikuta, S.; Kebarle, P. *J. Am. Chem. Soc.* **1984**, *106*, 6140.
(47) Holland, P. M.; Castleman, A. W. *J. Chem. Phys.* **1982**, *76*, 4195.
(48) Sunner, J.; Magnera, F.; Kebarle, P. *Can. J. Chem.* **1981**, *59*, 1787.
(49) Klots, C. E. *J. Phys. Chem.* **1988**, *92*, 5864.
(50) Kebarle, P.; Searles, S. K.; Zolla, A.; Scarborough, J.; Arshadi, M. *J. Am. Chem. Soc.* **1967**, *89*, 6393.
(51) Lau, Y. K.; Ikuta, S.; Kebarle, P. *J. Am. Chem. Soc.* **1982**, *104*, 1402.
(52) Hiraoka, K. *Can. J. Chem.* **1987**, *65*, 1258.
(53) Meot-Ner (Mautner), M. *J. Am. Chem. Soc.* **1978**, *100*, 4694.
(54) Castleman, A. W.; Holland, P. M.; Keesee, R. G. *Radiat. Phys. Chem.* **1982**, *20*, 57.
(55) Deakyne, C. A. *J. Phys. Chem.* **1986**, *90*, 6625.
(56) Wagman, D. D.; Evans, W. H.; Parker, V. B.; Schumm, R. H.; Halow, I.; Bailey, S. M.; Churney, K. L.; Nuttal, R. L. *J. Phys. Chem. Ref. Data* **1982**, *11* (Suppl. 2).
(57) Deakyne, C. A.; Meot-Ner (Mautner), M.; Campbell, C. L.; Hughes, M. G.; Murphy, S. P. *J. Chem. Phys.* **1986**, *84*, 4958.
(58) Wei, S.; Tzeng, W. B.; Castleman, A. W. *J. Phys. Chem.* **1991**, *95*, 585.
(59) Stace, A. J.; Moore, C. *J. Phys. Chem.* **1982**, *86*, 3681.
(60) Stace, A. J. *J. Am. Chem. Soc.* **1984**, *106*, 2306.
(61) Lias, S. G.; Liebman, J. F.; Levin, R. D. *J. Phys. Chem. Ref. Data* **1984**, *13*, 695.
(62) Meot-Ner (Mautner), M.; Sieck, L. W. *Int. J. Mass Spectrom. Ion Processes* **1991**, *109*, 187.
(63) Stull, D. R.; Westrum, E. F.; Sinke, G. S. *The Chemical Thermodynamics of Organic Compounds*; John Wiley: New York, 1969.
(64) Holland, P. M.; Castleman, A. W. *J. Phys. Chem.* **1982**, *86*, 4181.

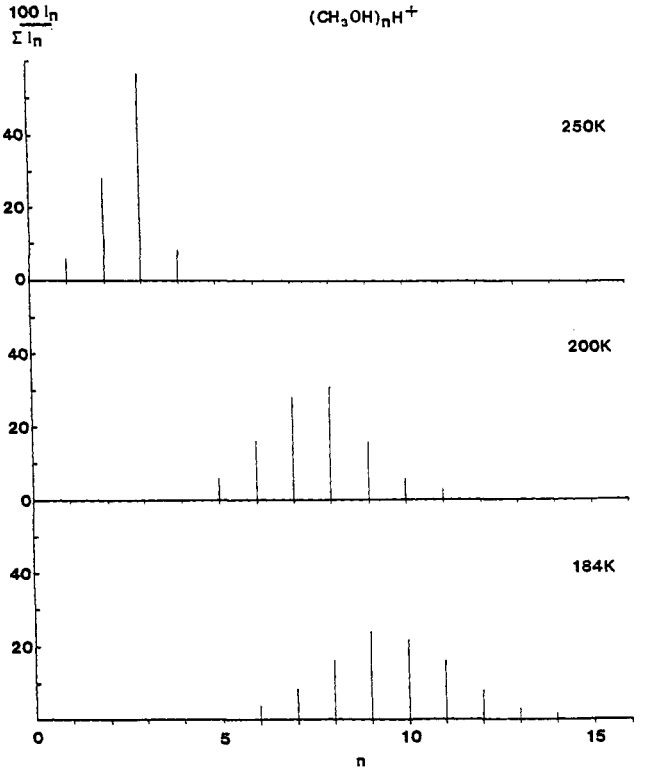

Figure 11. Equilibrium cluster ion distributions in 1% MeOH in N_2, $P(N_2)$ = 2.0 mbar at 250 K and 1.6 mbar at 200 and 184 K. Note the rapid shift to broad distributions and high clusters as the condensation temperature is approached. The neutral MeOH vapor at 184 K may be supersaturated.

with this, but measurements on larger clusters, using the collisional dissociation methods of Magnera et al., would be desirable.

Summary

Bonding to the core ions in the protonated organics appears to be dominated by distinct ionic hydrogen bonds, and alkyl group interactions do not contribute significantly. This is consistent with previous observations on dimer ions of hindered amines and pyridines,[20] which shows that hydrophobic alkyl–alkyl interactions contribute less than 8 kJ/mol (2 kcal/mol) to the bonding energies.

The transition to the outer shells is characterized by a drop of 17 ± 4 kJ/mol (4 ± 1 kcal/mol) in the bonding energies, regardless of the degree of alkylation. The constant value may be due to the opposing effects of intramolecular and intermolecular charge delocalization at the shell-filling step.

The limiting bonding energies in the outer shells do vary with alkylation, and $-\Delta H°_{n-1,n}$ approaches $\Delta H°_{evap}$. These trends suggest hydrophobic alkyl–alkyl interactions already in moderate size clusters of 5–10 molecules. The coincidence of $-\Delta H°_{n-1,n}$ with $\Delta H°_{evap}$ in a variety of clusters suggests compensating and/or small surface tension and dielectric terms at n = 6–10, in accord with continuum models, and the emergence of complex liquidlike structures and interactions. In hydrogen-bonded clusters, this corresponds to multiply bonded cyclic structures[54,55,58–60,65] and small atomic charges in the second and third shells. The approach to bulk condensation energies, in clusters where most molecules are on the surface, requires more theoretical work. In any event, large alkylated molecules behave in this respect similar to more simple molecules.

The present results suggest a structured hydrogen bond network in the inner shell and a more disorganized liquidlike structure in the outer shells. This seems to be carried over into the condensed phase. Diffraction and molecular mechanics studies show that the directional orientation of water molecules in the second shell about ions in solution is significantly smaller than in the inner shell.[68]

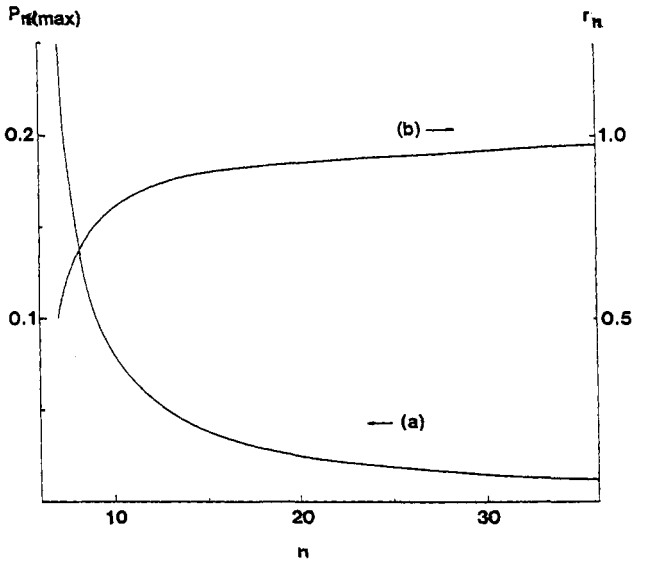

Figure 12. Relation among r_n, n, and $P_{n(max)}$. (a) As r approaches 1 (condensation), the population of each cluster n (normalized to the total population) goes through a maximum $P_{n(max)}$. The figure shows that the maximum population that cluster n can reach decreases with n. (b) Shows the value of r at which the nth cluster reaches its maximum population. Note that large clusters (n > 10) reach their maximum population when r is between 0.8 and 1, i.e., near condensation.

It would be of much interest to extend thermochemical studies on organic molecules to even larger clusters, but equilibrium studies are limited (see the Appendix). New methods[58,66] applied to organic clusters should reveal rich and complex behavior.

Acknowledgment. This work was supported by the Division of Chemical Sciences, Office of Basic Energy Sciences, U.S. Department of Energy.

Appendix

Cluster Distributions near the Condensation Limit. The present work is concerned with large clusters. The studies are limited by condensation on the ion source walls, which may have a smaller free energy barrier to condensation than the vapor, so that even the gas-phase homogeneous condensation temperature is hard to reach. Clusters of certain sizes may always be absent because of free energy barriers to condensation.[54] The equilibrium concentrations of those large clusters that are present are small, and they are observable over a narrow temperature range.

The following schematic and approximate arguments illustrate the experimental difficulty. The approximations are used to allow a general treatment, since in real clusters the thermochemistry varies from system to system. For example, in some systems the thermochemistry truly converges to constant values of $\Delta H°$ and $\Delta S°$, i.e., the van't Hoff plots converge,[23] while in others, the van't Hoff plots remain separated,[67] possibly because of increasingly negative $\Delta S°_{n-1,n}$ caused by steric crowding.

For the present schematic model, we will assume that the thermochemistry approaches a limiting value at some size N in each clustering sequence, and remains approximately constant for all $n > N$. An example is observed in the methanol sequence in Figure 9 where we can assign N = 7, and the thermochemistry remains approximately constant until n = 14.

(65) Newton, M. D.; Ehrenson, S. *J. Am. Chem. Soc.* **1971**, *93*, 4971. Newton, M. D. *J. Chem. Phys.* **1977**, *67*, 5535.

(66) Magnera, T. F.; David, D. E.; Michl, J. *Chem. Phys. Lett.* **1991**, *182*, 363.

(67) Hiraoka, K.; Mori, T.; Yamabe, S. *J. Chem. Phys.* **1991**, *94*, 2697.

(68) Heinzinger, K.; Palikas, G. In *The Chemical Physics of Solvation*; Dogonadze, R. R., Kalman, E., Kornyshev, A. A., Ulstrup, J., Eds.; Elsevier: Amsterdam, 1985; p 313.

(69) Hiraoka, K.; Mori, T. *Chem. Phys.* **1989**, *137*, 345.

(70) Wei, S.; Tzeng, W. B.; Castleman, A. W. *J. Chem. Phys.* **1990**, *93*, 2506.

The limiting thermochemical values can be denoted as $\Delta H°_{n-1,n} = \Delta H°_{lim}$ and $\Delta S°_{n-1,n} = \Delta S°_{lim}$, and the corresponding equilibrium constant is $K_{n-1,n} = K_{lim}$ for all $n > N$. In other words, the relative concentrations of each two consecutive clusters are the same for each cluster pair $n - 1$, n, independent of n. The cluster distribution is then a geometric series, and this allows a simple general treatment. Note that this model will ignore clusters smaller than the limiting size N. Even if present, they do not affect the equilibrium distribution among the larger clusters. Since we consider only the $n > N$ clusters, they may be indexed by i, so that $i = n - N$.

The relative equilibrium concentration r of any two consecutive clusters is given by eq 2 (P_M is the partial pressure of M). We consider temperature studies at constant pressure of M, i.e., at constant P_M. Note that, for all the clustering series, i.e., any value of $-\Delta H°_{lim}$ and $-\Delta S°_{lim}$, the values of r, and therefore the cluster distributions, will go through the same values, although at different temperatures.

$$r = [M_iH^+]/[M_{i-1}H^+] = P_M K_{lim} = P_M \exp(-\Delta H°_{lim} + T\Delta S°_{lim})/RT \quad (2)$$

If the concentration of the Nth cluster is C_N, then the concentration of any higher cluster i is $C_N r^i$. Note that K_{lim} and r are functions of the temperature. Above the condensation temperature, $r < 1$ and the concentration of large clusters vanishes with increasing i. Below the condensation temperature, $r > 1$ and the concentration of large clusters approaches infinity; i.e., condensation occurs.

The normalized population P_i of the ith cluster is given by eq 3.

$$P_i = C_i/\sum C_i = (1 - r)r^i \quad (3)$$

During a temperature study (at constant pressure), K_{lim} and the corresponding value of r change according to eq 2. Accordingly, as the temperature decreases, the population shifts to larger clusters, as in Figure 11. As to the population of a specific large cluster i, the population distribution first shifts toward it and then shifts toward even larger clusters. Therefore, the normalized population P_i of cluster i reaches a maximum value $P_{i(max)}$ at a certain temperature, i.e., a certain value r which is denoted as $r_{i(max)}$. The value of $r_{i(max)}$ is calculated by differentiating eq 3.

$$r_{i(max)} = i/(i + 1) \quad (4)$$

Substituting into eq 3 then yields the maximum normalized concentration that clusters of size i can reach.

$$P_{i(max)} = i^i/(i + 1)^{(i+1)} \quad (5)$$

The maximum normalized population that cluster i can assume decreases with i, approximately as $1/i$.

Figure 12 shows that any cluster with a large n can constitute only a small fraction of the total population at any value of r, i.e., at any temperature. For large clusters, this small maximum population is realized when r is near 1, which is near the condensation temperature.

For example, we use $\Delta H°_{lim} = -36$ kJ/mol (-8.6 kcal/mol) and $\Delta S°_{lim} = -105$ J/(mol K) (-25 cal/(mol K)) for $(MeOH)_nH^+$, and these values apply for $n > 8$. At a typical experimental partial pressure of $P(MeOH) = 0.02$ mbar, the value of $r = [(MeOH)_nH^+]/[(MeOH)_{n-1}H^+]$ becomes unity, i.e., condensation in the cluster ion series occurs, at 182 K (note that the neutral vapor may also be supersaturated under these conditions). Just above this temperature, $r < 1$, and P_n vanishes at large n. For example, 6 °C above the condensation temperature, $r = 0.5$ and the population of any cluster with $n > 11$ constitutes less than 5% of the total ion population. Applying eq 4 to this example shows that the concentration of any cluster with $n > 14$ is always less than 5% of the total cluster population. Furthermore, these large clusters have observable concentrations only in a short temperature interval.

In summary, near condensation the neutral vapor itself may partially cluster and partially condense, making the vapor pressure uncertain. As to the ion clusters, the concentrations of the large clusters constitute approximately a decreasing geometric series. Large clusters are present only in small concentrations at any temperature, and are observable only in a narrow temperature range. In fact, as the cluster size n approaches infinity, the temperature range over which it is observable becomes infinitesimally small.

These constraints make temperature studies, and for larger clusters even equilibrium measurements at a single temperature, impractical. This is why our $(MeOH)_nH^+$ series ends at $n = 14$. The largest cluster for which van't Hoff plots have been published to date is $n = 18$ in $(CO)_{18}^+$.[67]

Registry No. MeOH, 67-56-1; PrOH, 71-23-8; $CH_3(CH_2)_4OH$, 71-41-0; CH_3CO_2H, 64-19-7; $MeNH_2$, 74-89-5; $PrNH_2$, 107-10-8; Me_2NH, 124-40-3.